

Towards Marine Bloom Trajectory Prediction for AUV Mission Planning

Jnaneshwar Das*, Kanna Rajan[†], Sergey Frolov[†], Frederic Py[†], John Ryan[†], David A. Caron[‡], Gaurav S. Sukhatme*

*Robotic Embedded Systems Laboratory and Dept. of Computer Science, University of Southern California

[†]Monterey Bay Aquarium Research Institute, Moss Landing, California

[‡]Dept. of Biological Sciences, University of Southern California

jnaneshd@usc.edu, {kanna.rajan,frolovs,fpy,ryjo}@mbari.org, dcaron@usc.edu, gaurav@usc.edu

Abstract—This paper presents an offshore oceanographic toolchain that can be used to generate survey missions for multi-vehicle robotic surveys for large-scale dynamic features in the coastal ocean. Our science application targets Harmful Algal Blooms (HABs) which have significant societal impact to coastal communities yet are poorly understood in terms of their ecology. Since bloom patches can be large (kms) and unpredictable in their movement, to understand their evolution, we need to be able to bring back water samples from the 'right' places and times, for lab analysis. In doing so, we target hotspots (representative of intense biogeochemical activity) for such sampling. Our approach uses remote sensing data to detect such hotspots using ocean color as a proxy, and advectively projects these patches spatio-temporally using surface current data from HF Radar stations. Experiments with satellite and Radar data sets are promising for large, coherent blooms. We show how these predictions can be used to select an appropriate lawnmower sampling trajectory for an AUV.

I. INTRODUCTION

Observing large scale oceanographic features has often been difficult. For example Intermediate Nepheloid Layers are near-coastal features which are fluid sheets of suspended particulates with large horizontal extent (in Kms) and small vertical extent (in 1-10 meters). Harmful Algal Blooms (the focus of this paper) are likewise spread over Kilometers with primary productivity driving its ecology within the top 5-10 meters. Traditional approaches using ship-based measurements for observing such dynamic and episodic phenomenon have proven to be ineffective given evolving biological state, the need to measure various properties across the spatial extent of such phenomenon and most of all in dealing with logistical details centered on manned ships which are on fixed schedules.

More recently Autonomous Underwater Vehicles (AUVs) have shown to be more cost-effective, have demonstrated increased persistent presence and with a suitable sensor payload have been able to systematically observe large scale phenomenon at requisite scales of variability of biogeochemical processes which drive such phenomenon. Yet often such mobile robotic assets have been ineffective in resolving the spatio-temporal characteristics to effectively sample and observe. Additionally while satellite observations have proven to be helpful, they are constrained either by cloud cover, the lack of data beyond a meter or two of the sea surface when process driven phenomenon can and are often within the euphotic zone (upto 150m) and logistical issues with the time lag between observations and processed data sets available for use. Mooring data suffers from a spatial

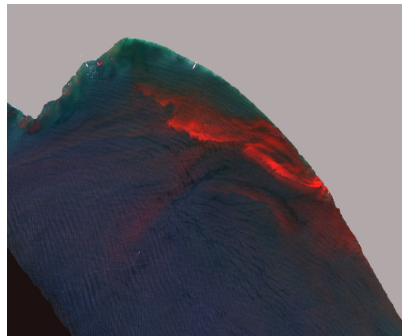


Fig. 1. NIR-G-B composite image of NE Monterey Bay on August 26, 2004, when an extremely dense red tide bloom was present.

sparseness even if in-situ measurements are accurate and available in real-time.

Our goal and the subject of this paper is to make use of the data available from a range of sources including ocean models, remote sensing satellites, moorings, and on-shore instruments to make predictions of the trajectory of a patch of water. We target HABs for a number of reasons.

One type of HAB causes reddish discoloration of surface waters which are visible in ocean color remote sensing data. An image of a red tide bloom in NE Monterey Bay is shown in Fig. 1. These blooms are caused by dinoflagellates, which comprise 75% of all HAB species. Dinoflagellates can form extremely dense aggregations, and if the species is toxic, their aggregation can make transfer of toxins into the food web much more efficient and harmful. Ocean physics occurring on small scales can contribute to the dense aggregation of red tide blooms [1]. The red tide image in Fig. 1 shows a narrow band of extremely high near-infrared reflectance (a characteristic signature and a basis for quantifying bloom intensity). Infrared imaging showed that this high-intensity bloom band was in a thermal frontal zone. The causes and triggers for these blooms vary depending upon regional characteristics and the ocean current system.

To understand the bloom ecology (why and when they occur, and why they decay), it is necessary to sample bloom hotspots with high spatio-temporal resolution. Hotspots are regions in the bloom with very high biochemical activity substantially driving bloom ecology. To plan survey missions, scientists rely on satellite imagery, data from moorings and drifters, ocean models, and seasonal patterns in observing HABs with the goal to maximize the likelihood of sampling hotspots as well as to be able to stay with a patch of the water with such intense activity. However, as mentioned earlier, predicting the occurrence of a bloom is a difficult task given the complex variability in coastal waters coupled with

rudimentary understanding of phytoplankton ecology [2]. Because of the non-localized nature of blooms, the size of the observation area, and the lack of understanding of the exact dynamics, ship-based and AUV missions often under-sample bloom hotspots. Factors negatively impacting mission success include the lag in obtaining processed satellite data (usually 1-2 days), and the spatial sparsity of mooring data. Additionally, plans are made in an ad-hoc, per deployment basis and cannot be generalized to be used in a continuous, repeatable manner.

In this paper, we address the problem of planning sampling missions for observing HABs. We address a piece of the larger problem: how to predict the trajectory of an algal hotspot. As robotics technologists, our aim then is to design sampling surveys as a means to decide whether one or more robotic asset will sufficiently sample; when more than one asset, where to deploy such assets given the large spatial extent of blooms and finally to motivate design of intelligent coordination algorithms when multiple assets are deployed and to ensure such configurations are robust to the harsh environmental conditions.

Our paper is organized as follows. Section II gives a brief overview of data sources, the key projection algorithms and motivations for using these approaches. In section III we analyze the results of our experiments and follow it up with sample AUV survey designs in section IV. Finally we conclude our findings and briefly articulate future work in section V.

II. SYSTEM DESCRIPTION

The dynamics of an algal bloom can be primarily described by three factors: advection, diffusion, and bloom ecology. Advection is the component of the transport that is due to the effect of external forcing (ocean current). Diffusion results from movement of particles along concentration gradients. Lastly, since the phenomenon is biological, its growth and decay is governed by bloom ecology. To predict the dynamics of the bloom for long timeframes (*e.g.*, months) would require data for all three factors described above. However, for a strong coherent bloom already in progress, predictions can be made for a period of upto a week based on the external forcing and diffusion. Ocean observing systems such as SCCOOS [3] and CeNCOOS [4] provide near-realtime data on various aspects of the physical sea-state such as temperature, current, salinity and sea surface height. JPL's Regional Ocean Modeling System (ROMS) [5] model for the Southern California Bight region generates forecasts for these physical properties. Given access to these data, we ignore ecology and diffusion and focus on the advective effect of ocean currents on blooms. In [6], [7], gliders were used to track fresh water plumes based on ocean current predictions from JPL's ROMS model. [1] discusses the effect of external forcing on blooms occurring in the Monterey Bay. Monterey Bay is one of the most biologically diverse bodies of waters in the world. The Northeast Monterey Bay frequently experiences extreme "red-tide" blooms, making it an ideal location for studying the prediction of algal

blooms. In this paper, we analyze the result of advecting hotspots from blooms that occurred between October 2007 and October 2008 at the Monterey Bay. Finally, we show an example of how such predictions can be used to plan simple survey missions for AUVs.

Our system computes prediction of bloom trajectories in two steps,

- 1) patches of bloom hotspots are detected from remote sensing data,
- 2) detected patches are advected using surface current data from HF Radar stations.

In this section we first discuss the data sources and then describe how we perform these two steps.

A. Data Sources

1) *Remote Sensing Data:* Remote sensing satellites provide a synoptic view of the oceans. Owing to the fact that phytoplankton have chlorophyll and are photosynthetic, ocean color and emitted radiance due to fluorescence are good proxies for chlorophyll concentration in the upper column of water¹.

Moderate Resolution Imaging Spectroradiometer (MODIS) [8] is a key instrument aboard the Terra and Aqua satellites that acquire data in 36 spectral bands. Terra's orbit around the Earth is timed so that it passes from north to south across the equator in the morning, while Aqua passes south to north over the equator in the afternoon. Terra MODIS and Aqua MODIS view the entire Earth's surface every 1 to 2 days.

One of the data products from the Terra MODIS satellite is Fluorescence Line Height (FLH). It is a relative measure of the amount of radiance leaving the sea surface in the chlorophyll fluorescence emission band (670nm) [9], [10].

There are instruments aboard other satellites that provide different data products that are indicators of upper column chlorophyll concentration. An example is the Sea-viewing Wide Field-of-view Sensor (SeaWiFS) and the chlorophyll-a data product. Fig. 2 shows a strong bloom in the Monterey Bay that occurred between September and October 2002.

MODIS data are available in Hierarchical Data Format (HDF). The FLH data product from each MODIS image is read into a 500 x 667 matrix I , where each cell represents the FLH value for a 0.25km x 0.35km area in the sea.

2) *High Frequency Radar Data (HF Radar):* To determine the trajectory of a bloom patch, we ignore diffusion and bloom ecology and focus only on the advective effect on a bloom hotspot. External forcing by wind and water currents is a dominating factor in bloom transport and we expect to get reasonable estimates of the trajectory of hotspots over a period of few days using only external forcing. We used surface current data obtained from HF Radar stations maintained by CeNCOOS. HF Radar provides radial ocean surface current information in near-real time. With data from multiple HF Radar stations, the velocity components of the surface current is computed. The data must be filtered,

¹the volume of water < 6-10m in depth

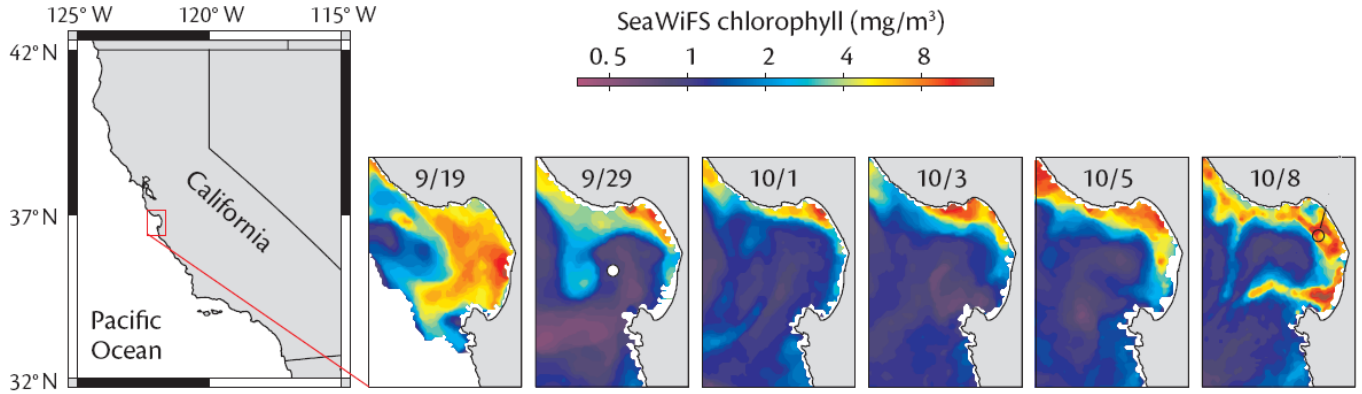


Fig. 2. SeaWiFS images showing a red-tide bloom at the Monterey Bay between September and October 2002 (source: Coastal Ocean Physics and Red Tides: An example from Monterey Bay, California)

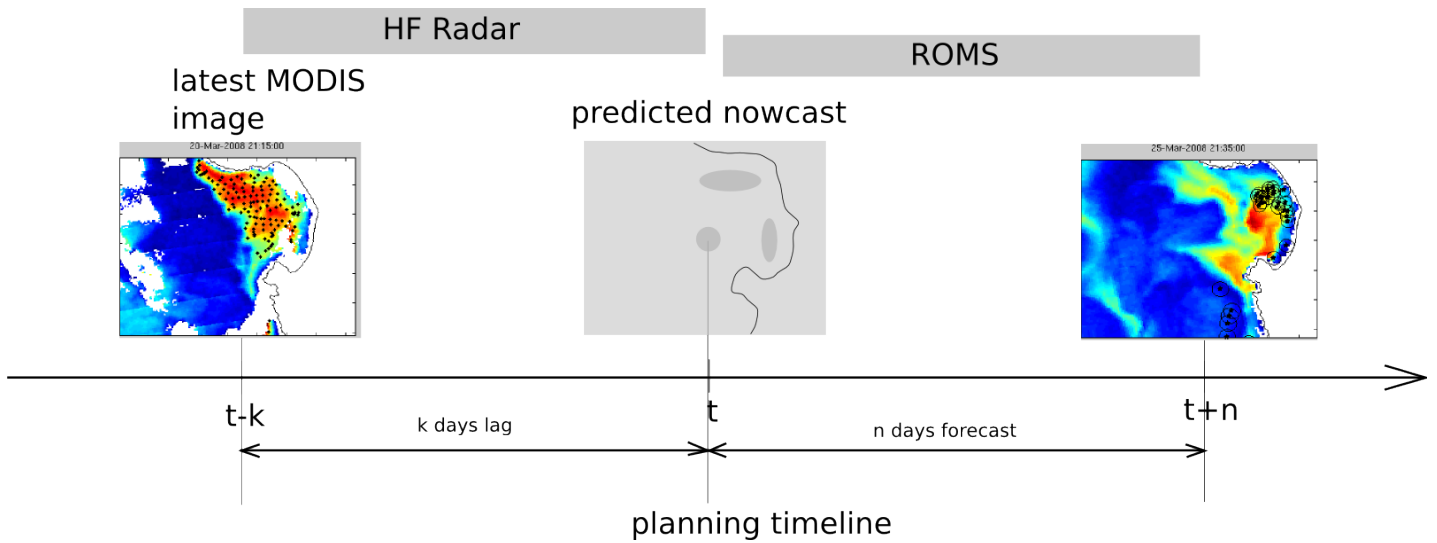


Fig. 3. Illustration of a scenario where a satellite image is obtained with a lag. HF Radar data is used to generate prediction of bloom locations. ROMS forecast of ocean current can be used to generate predictions into the future for bloom locations.

interpolated and extrapolated. we obtained Open-Boundary Modal Analysis (OMA) interpolated HF Radar data for the period October 2007 - October 2008 from CeNCOOS. With the lack of a predictive ocean model such as ROMS for the Monterey Bay region, we did not have forecasts on the surface currents. However, since our analysis is on archived data to validate bloom projection results, we did not require forecast of surface current. The work presented in this paper can be used with ROMS model surface current projections as in [7] where the authors used ROMS model projections to track a fresh water plume using 48 hours surface current projections. Figure 3 illustrates the data sources and the time-line of predictions.

B. Hotspot trajectory prediction

1) *Hotspot detection*: We define a bloom hotspot as the region of the MODIS FLH images that has values greater than a threshold F . Given the MODIS FLH images, we first threshold each image above F to obtain the high intensity

patches. The thresholded image may contain many small disconnected regions. Since, we are interested in tracking patches that are of significant size, we detect large patches by finding all thresholded regions that have a connectivity of 8. Since each point being advected has to go through multiple timesteps, doing this for all the points within a patch is time consuming. Hence, once we have the bloom patches or 'hotspots', we need to choose representative points within the patch that want to advect. We can advect just the centroid of each patch, points from the convex hull, the boundary, or from within the patch. In this paper, we choose points sampled uniformly at a desired resolution from within each patch. These sample points represent a lower resolution representation of the hotspot that can be advected using the surface current data.

2) *Hotspot advection*: The sample points within the patch are advected using surface current data available obtained from CeNCOOS. Hourly HF Radar data are available at a 2 Km resolution in a gridded format. We first interpolate the

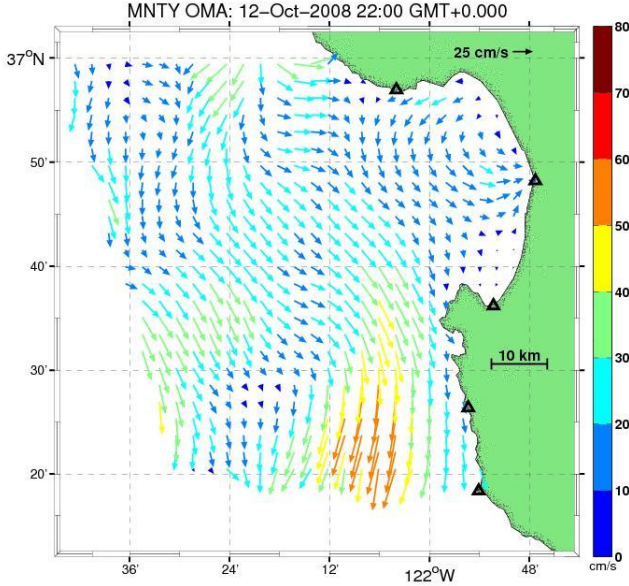


Fig. 4. Open Normal Mode Analysis (OMA) modeled hourly current vectors for the Monterey Bay (source: CeNCOOS)

data such that for any location p , and time t , we have

$$R_{p,t} = \begin{bmatrix} u \\ v \end{bmatrix}. \quad (1)$$

where u and v are the surface current velocity components along X (east) and Y (north) axes respectively. A sample point p is defined by the geographical location in i.e., longitude x and latitude y , and the corresponding FLH value f :

$$p = \begin{bmatrix} x \\ y \end{bmatrix}. \quad (2)$$

where u and v are the surface current velocity components along X (north) and Y (east) axes respectively. The sample point is hence defined by,

$$s = \begin{bmatrix} p \\ f \end{bmatrix} \quad (3)$$

We perform a kinematic projection of a sample point using the HF Radar velocity estimates. For each point p within a patch, we project its evolution by use of,

$$p_{t+1} = p_t + R_{p,t+1} \Delta t. \quad (4)$$

The error covariances for the OMA velocity estimates are available as σ_u and σ_v for each data point in the grid. We use this to additionally project the error on the estimate of the advected point location. Since we are doing a kinematic projection, each point undergoes a linear transformation. The new error in the location can hence be obtained by simply adding the previous error to the new error associated with a one-step projection:

$$\sigma_{p_{t+1}} = \sigma_{p_t} + \sigma_{R_t} \Delta t. \quad (5)$$

Algorithm 1: hotspot detection and advection algorithm

```

1 Input: MODIS images  $M_1$  and  $M_2$ 
2 Time period  $T = \text{timestamp}(M_2 - M_1)$ 
3  $t = t_{M_1}$ 
4  $I_{\text{thresholded}} = \text{threshold}(M_1, F)$ 
5  $H = \text{connectedSegments}(I_{\text{thresholded}}, 8)$ 
6  $h$  hotspots,  $H = \{H_1, H_2, \dots, H_h\}$ 
7 foreach HotSpot  $h_i$  do
8   sample points for HotSpot  $h_i$ ,
9    $P_i = \text{resampleHotspot}(h_i, \text{resolution})$ 
10   $P_i = \{p_1, p_2, \dots, p_N\}$ 
11  foreach sample point  $p_j = [x, y, t]$  do
12    while  $t < t_{m2}$  do
13       $R_{p,t} = [u, v]'$ 
14       $p_{t+\Delta t} = p_t + R_{p,t} \Delta t$ 
15       $\sigma_{p_{t+1}} = \sigma_{p_t} + \sigma_{R_t} \Delta t$ 
16       $t = t + \Delta t$ 
17    end
18  end
19 end

```

The pseudocode for the detection and advection of bloom patches is presented in Algorithm 1

In our current implementation, we do not model error in FLH estimates of the projected bloom. We retain the original FLH value for each sample point throughout the advection. This error will be present because our approach does not consider diffusion and bloom ecology. However, this is not restrictive for our application, and can be modeled as a Gaussian error that grows exponentially with time. We also assume that the surface current field is constant within the neighborhood of the advected point. Without this assumption, Equation 5 will not hold true.

III. ANALYSIS AND RESULTS

We performed advection of FLH hotspots on a dataset of MODIS FLH images captured between September 2007 and November 2008. The period was chosen such that we had both MODIS and HF Radar data. MODIS images are often unusable due to cloud cover or corrupted images. After rejecting the unusable images, we selected those that displayed hotspots of considerable intensity. We were also interested in studying the quality of the advection for different time periods. From the test cases, we identified 1, 2, 3, 4, and 5 day periods between MODIS images to ground truth our projections. In total, we selected 16 test cases spanning Fall 2007 to Fall 2008.

The resulting projections were evaluated qualitatively by a physical oceanographer. The following table shows the results of our evaluation. We observed good predictions for stronger blooms, specifically blooms in Fall. The advection of bloom patches fail to predict blooms that are in the initial stages of growth. The projections were good for blooms that were well developed and of high intensity.

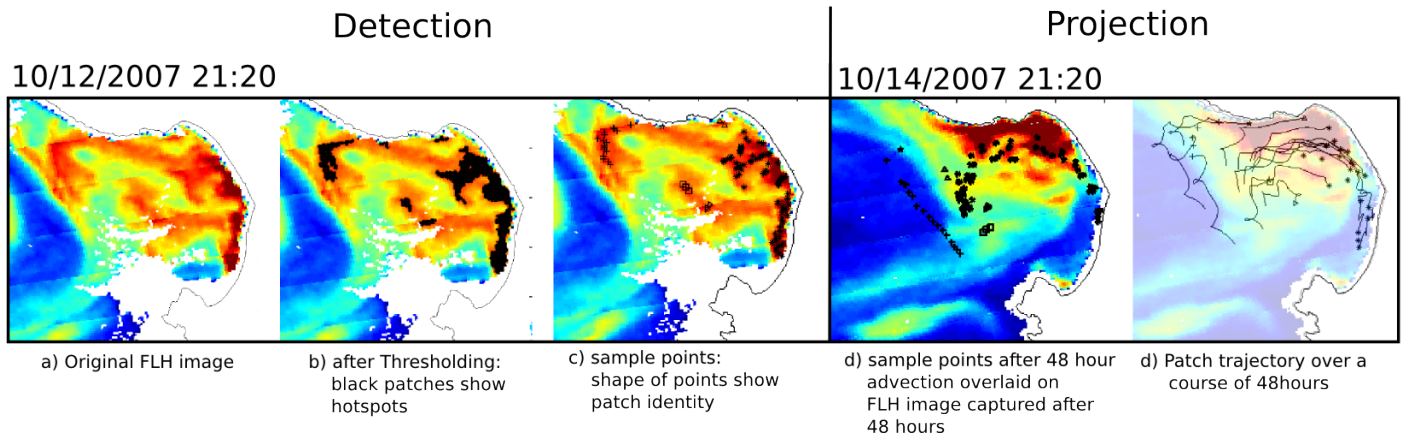


Fig. 5. Projection of a bloom from October 2007.

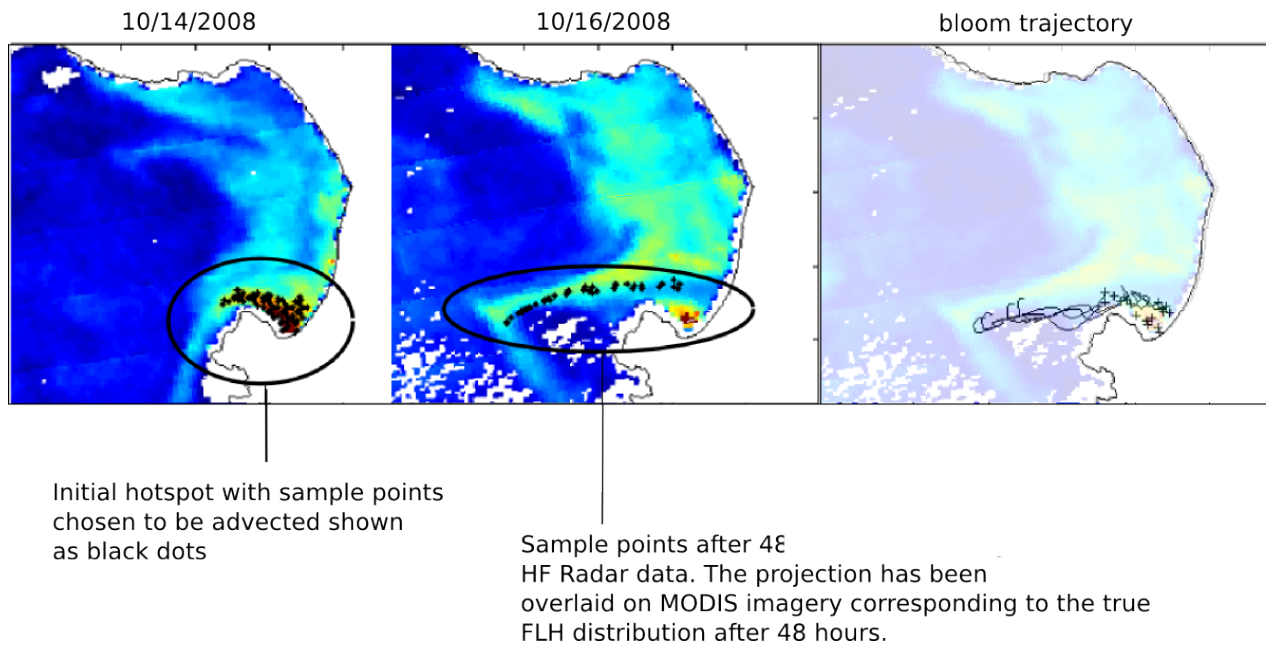


Fig. 6. Projection of a bloom from October 2008.

Hotspot Projection Test Cases		
Period(days)	Case	Evaluation Rating (max 5)
5	03/20/2008	3
4	06/02/2008	4
	10/12/2008	4
3	10/09/2008	4
2	10/12/2007	4.5
	02/15/2008	3
	03/18/2008	2
	03/25/2008	2
	04/10/2008	2
	04/26/2008	2
	05/21/2008	3
	10/10/2008	3.5
1	10/12/2008	3
	10/14/2008	5
	10/24/2007	4
	10/09/2008	2

Figures 5 and 6 show a couple of two-day projections from the 16 evaluated test cases.

IV. AN APPLICATION IN AUV SURVEYING

Based on the prediction of hotspot trajectory, we wish to choose the best survey area for an AUV. A compelling scenario for such an application is illustrated in Figure 7: We have satellite data that is two days old showing an ongoing bloom. We wish to plan an AUV survey based on this data that will allow us to be at the best possible location to sample the bloom hotspot. We run the trajectory projection algorithm to obtain a nowcast on the bloom using HF Radar data. Note that even without ROMS forecast, we usually have access to current HF Radar data that can be used for the above scenario. Next, we describe the determination of the survey parameters.

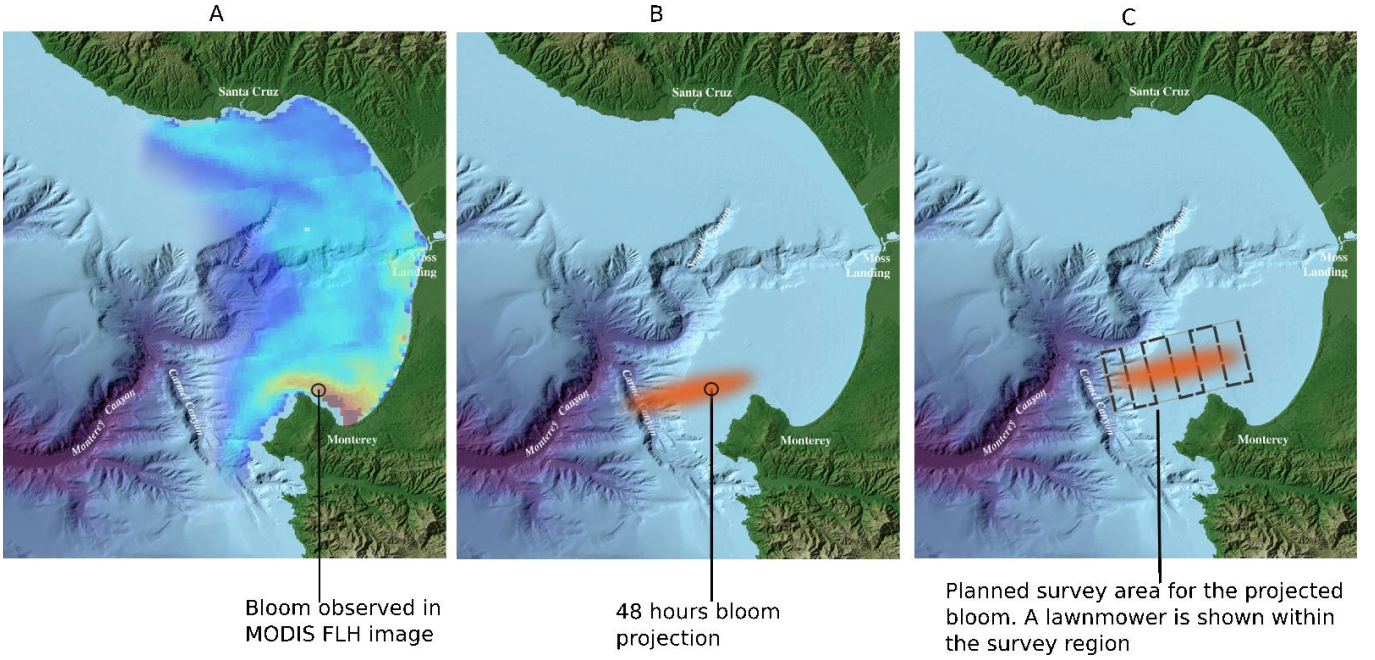


Fig. 7. The illustration of an offshore planning toolchain. This paper focuses on the generation of bloom trajectories that can be used to plan survey missions.

A. Survey template

The lawnmower or radiator pattern is among the most widely used survey pattern in oceanography because of its uniform coverage and resulting ease of visualization. We design our solution with the lawnmower as the desired survey template, based on the constraints on the AUV *i.e.*, the runtime and the nominal velocity. Let the maximum runtime be T and the nominal velocity be v_{AUV} . The maximum distance that the AUV can cover is given by,

$$L_{AUV} = Tv_{AUV} \quad (6)$$

We define a lawnmower pattern with the sides a and b and the swath width w . total length of the lawnmower is given by,

$$L = \left(\frac{a}{w} + 1\right)b + a, \quad (7)$$

$$L = \frac{ab}{w} + (a + b), \quad (8)$$

$$L = k_1 \cdot A + k_2 \cdot P, \quad (9)$$

where A and P are the area and perimeter respectively of the bounding rectangle, $k_1 = 1/w$, and $k_2 = 1/2$. The bounding-box for the lawnmower is given by rectangle R , defined by the center p_c , sides a and b , and the angle θ the bounding box makes with the x-axis. We assume that the parameters of the bounding box that defines the survey area are predecided. In Equation 9, we see that the length of the lawnmower pattern is a linear combination of the area and perimeter of the bounding box. So by choosing the sides of the bounding box, we can implicitly constrain the length of the lawnmower. In later versions, we will relax this constraint and find the lawnmower that maximizes the reward with constraint only on the length.

The information content can be chosen to be the signal variation (captured by the Hessian), or the signal strength. Since our goal is to attain maximum spatio-temporal sampling resolution at hotspots, we want to maximize the total signal intensity in the region where we sample. AUVs are equipped with a suite of *in-situ* sensors that can sample additional parameters of interest in these regions where the expected chlorophyll concentration is high. We define the survey quality of our sampled region as the total signal intensity within the survey area.

For a candidate survey area bounded by rectangle R , the sampling reward is given by

$$r = \sum_{i=0}^n e^{\alpha f_i} \cdot g_R(p_i) \quad (10)$$

where α is a chosen constant, g is given by,

$$g(p) = \begin{cases} 1, & \text{if } p \text{ is inside rectangle } R \\ 0, & \text{if } p \text{ outside rectangle } R \end{cases} \quad (11)$$

The weighting function over FLH was chosen to be exponential to reward higher values of FLH favorably.

Given a survey layout of known dimension, we want to determine the best location and orientation for the survey. To achieve this, we use the nested grid approach to search for the location and orientation of the survey area that maximizes the reward described by 10. For our test case, we choose the length of the sides of the survey rectangle given by a and b as 16km and 5km respectively.

To find the best location and orientation for the survey-area, we use the following approach. First, we find the bounding box of the projected sample points. This gives us the region of the ocean that has the maximum likelihood of

an ongoing bloom based on our projection algorithm. On this bounding box, we perform a recursive grid search. In each step, we split the bounding box into a 4x4 grid and compute the reward for each cell using Eqn(10). We select the cell that has maximum reward, and continue the process. The recursion is terminated when the subsequent grid size is smaller than the survey area size. At this stage, we do an exhaustive search in the final cell (which would be larger than the survey-area since the grid search is terminated) to define the location and orientation of the survey-area.

Figures 8 and 9 show the result of our search algorithm on the example bloom cases from October 2007 and 2008. The dotted box shows the initial bounding box and the solid box shows the final survey area chosen by the search algorithm.

Algorithm 2: recursiveBestGrid(G,a,b)

```

1 Input: survey area parameters  $a$  and  $b$ 
2 grid  $G$ 
3  $L$  and  $B$  are length and breadth of bounding-box  $B$ 
4 if  $L/2 < a$  OR  $B/2 < b$  then
5   return  $G$ 
6 end
7  $L = L/2, B = B/2$ 
8  $m = \arg \max_i (\text{samplingReward}(G_i, P))$ 
9 recursiveBestGrid( $G_m, a, b$ )

```

Algorithm 3: findSurveyArea(P,a,b)

```

1 Input:  $N$  projected sample points  $P = \{p_1, p_2, \dots, p_N\}$ 
2 survey area parameters  $a$  and  $b$ 
3 bounding-box of advected points  $B$ 
4  $G_{max} = \text{recursiveBestGrid}(B, a, b)$ 
5  $[S_p, \theta] = \text{findBestArea}(G_{max}, a, b)$ 

```

Figures 8 and 9 show the results of our search on the bloom cases from October 2007 and October 2008.

V. CONCLUSION AND FUTURE WORK

This paper presents an offshore oceanographic toolchain that can be used to generate survey missions for Autonomous Underwater Vehicles (AUVs). The approach uses remote sensing data to detect algal hotspots, and projects these patches advectively using surface current data from HF Radar stations along the central California coast. Result of advecting hotspots from blooms that occurred between October 2007 and October 2008 are promising for large, coherent blooms. Finally we show an example of how such predictions can be used to plan simple (lawnmower pattern) survey missions for AUVs. In the future we plan to incorporate diffusion into the model and investigate irregular sampling methods.

VI. ACKNOWLEDGMENTS

This work was supported in part by the NOAA MERHAB program under grant NA05NOS4781228 and by NSF as part of the Center for Embedded Network Sensing (CENS) under

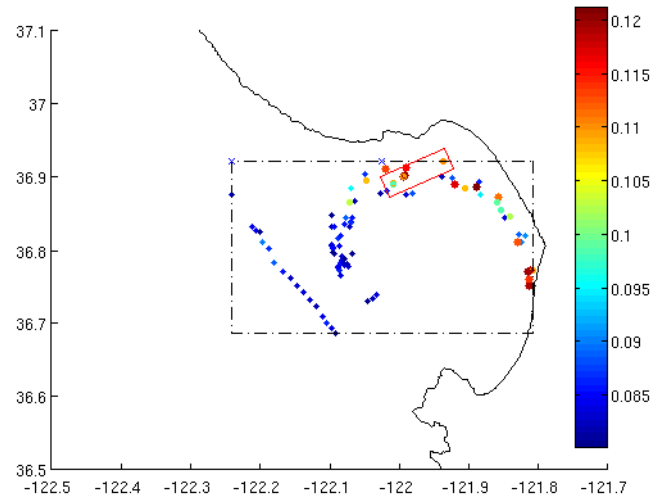


Fig. 8. Rectangular survey area of known size that maximizes the contained FLH intensity of the bloom case 1 (10/12/2007). The nested grid approach was used to search for the location and orientation of the rectangle that maximized the gain (FLH intensity).

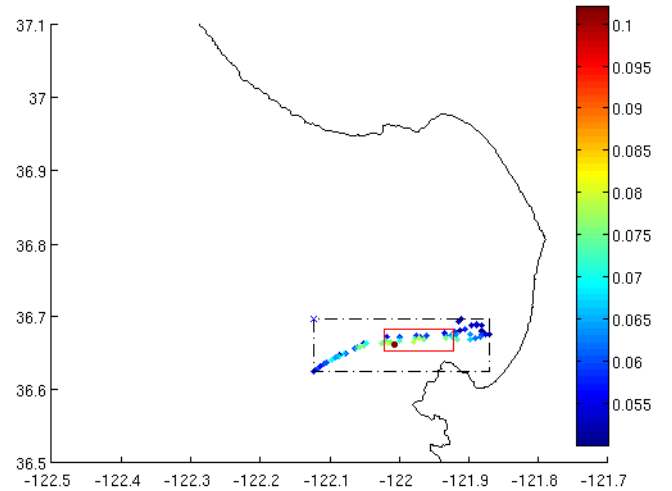


Fig. 9. Plot showing the survey rectangle for October 2008 bloom

grant CCR-0120778, by NSF grants CNS-0520305 and CNS-0540420, by the ONR MURI program (grants N00014-09-1-1031 and N00014-08-1-0693) by the ONR SoA program and a gift from the Okawa Foundation. We thank the David and Lucile Packard Foundation for supporting our work at MBARI.

REFERENCES

- [1] J. P. Ryan, H. M. Dierssen, R. M. Kudela, C. A. Scholin, K. S. Johnson, J. M. Sullivan, A. M. Fischer, E. V. Rienecker, P. R. McEnaney, and F. P. Chavez, "Coastal ocean physics and red tides: an example from monterey bay, california," *Oceanography*, vol. 18, pp. 246–255, March 2005.
- [2] J. P. Ryan, A. M. Fischer, R. M. Kudela, J. F. Gower, S. A. King, Marin, and F. P. Chavez, "Influences of upwelling and downwelling winds on red tide bloom dynamics in monterey bay, california,"

- Continental Shelf Research*, vol. 29, no. 5-6, pp. 785–795, March 2009. [Online]. Available: <http://dx.doi.org/10.1016/j.csr.2008.11.006>
- [3] “The The Southern California Coastal Ocean Observing System (SCCOOS).” [Online]. Available: <http://www.sccoos.org/>
- [4] “The Central and Northern California Ocean Observing System (CeNCOOS).” [Online]. Available: <http://www.cencoos.org/>
- [5] A. F. Shchepetkin and J. C. McWilliams, “The regional oceanic modeling system (roms): a split-explicit, free-surface, topography-following-coordinate oceanic model,” *Ocean Modeling*, vol. 9, pp. 347–404, 2005.
- [6] I. Cetinic, B. H. Jones, M. A. Moline, and O. Schofield, “Resolving urban plumes using autonomous gliders in the coastal ocean,” *Journal of Geophysical Research/American Geophysical Union*, 2008.
- [7] R. N. Smith, Y. Chao, B. H. Jones, D. A. Caron, P. P. Li, and G. S. Sukhatme, “Trajectory design for autonomous underwater vehicles based on ocean model predictions for feature tracking,” in *Proceedings of the International Conference on Field and Service Robotics*, Jul. 2009.
- [8] “Moderate Resolution Imaging Spectroradiometer (MODIS).” [Online]. Available: <http://modis.gsfc.nasa.gov/>
- [9] X.-G. Xing, D.-Z. Zhao, Y.-G. Liu, J.-H. Yang, P. Xiu, and L. Wang, “An overview of remote sensing of chlorophyll fluorescence,” *Ocean Science Journal*, vol. 42, pp. 49–59, March 2007.
- [10] R. M. Letelier and M. R. Abbott, “An analysis of chlorophyll fluorescence algorithms for the moderate resolution imaging spectrometer (modis),” vol. 58, pp. 215–223, 1996.